

1 A proof-of-principle study for $\delta^{15}\text{N}$ measurements of aqueous
2 dissolved nitrate and nitrite with a modified LC-IRMS
3 interface
4

5 Tobias Hesse^{1,5}, Felix Niemann¹, Shaista Khaliq¹, Daniel Köster⁴, Julian Enss², Christian
6 Feld^{2,3}, Milen Nachev^{2,3}, Klaus Kerpen¹, Maik A. Jochmann^{1,3}, Torsten C. Schmidt^{1,3}

7
8 ¹Instrumental Analytical Chemistry, University of Duisburg-Essen, Universitätsstr. 5, 45141
9 Essen, Germany

10 ²Aquatic Ecology, Faculty of Biology, University of Duisburg-Essen, Universitätsstraße 5,
11 Essen, 45141, Germany

12 ³Centre for Water and Environmental Research, University of Duisburg-Essen, Universitätsstr.
13 5, 45141 Essen, Germany

14 ⁴Institut Für Arbeitsschutz der Deutschen Gesetzlichen Unfallversicherung (IFA), Alte
15 Heerstraße 111, 53757 Sankt Augustin, Germany

16 ⁵Landesamt für Natur, Umwelt und Verbraucherschutz NRW, Wuhanstr. 6, 47051 Duisburg,
17 Germany

18
19 **Abstract**

20 **Rationale:**

21 The analysis of nitrogen isotopes in aqueous dissolved nitrate is an effective method for
22 identifying pollution sources and offers the potential to study the nitrogen cycle. However, the
23 measurement of nitrogen isotope signatures of nitrate still requires extensive sample preparation
24 or derivatization.

25 **Methods:**

26 In this study, a modified commercially available liquid chromatography-isotope ratio mass
27 spectrometer (LC-IRMS) interface is presented that enables automated measurement of $\delta^{15}\text{N}$
28 signatures from nitrate by online reduction of nitrate in two consecutive steps. First,
29 vanadium(III)-chloride is used as a reducing agent to convert NO_3^- to N_xO_y under acidic
30 conditions. The mix of nitrogen oxides is then transferred into a stream of helium and reduced
31 to nitrogen (N_2) analysis gas via a hot copper reactor. Prior to the online conversion of aqueous

32 nitrate into elemental nitrogen, the sample was chromatographically separated from potential
33 matrix effects on a PGC column.

34 **Results:**

35 Precision was achieved at a level below 1.4 ‰ by injecting 10 µL of 50 mg L⁻¹ N, using five
36 different nitrate standards and reference materials. These materials spanned a range of more
37 than 180 ‰ in δ¹⁵N. To demonstrate the applicability of the method we measured water samples
38 from an enrichment experiment, where isotopically enriched ammonium chloride was
39 administered into a small river over the course of two weeks. In contrary to our expectation, the
40 δ¹⁵N values of river nitrate showed values between +0.4 ± 0.4 ‰ and +4.1 ± 0.3 ‰, varying
41 over a small range of 3.7 ‰.

42 **Conclusions:**

43 Our study showed that the measurement of nitrate nitrogen isotope signatures with a modified
44 LC-IRMS system is possible, but that further modifications and improvements would be
45 necessary for a robust and user-friendly instrument.

46

47

48 **1 Introduction**

49 The main inorganic nitrogen species in rivers are ammonium, nitrite and nitrate. ¹
50 Contamination of water by anthropogenic nitrate has become a global environmental concern
51 and the measurement of nitrogen isotope ratios of nitrate is an effective method for identifying
52 and differentiating between natural and anthropogenic nitrate sources and it provides
53 opportunities to study the nitrogen cycle. However, established methods for determining the
54 nitrogen isotopic composition of nitrate at natural abundance levels are demanding and often
55 hinder rapid and reliable measurements required in water monitoring programs. A variety of
56 methods is used for the determination of the nitrogen isotope signature of nitrate in water:

57 (i) The ion-exchange method represents the earliest developed approach and employs an anion-
58 exchange column for the preconcentration of nitrate and nitrite. They are then removed from
59 the column by hydrochloric acid and analyzed as silver nitrate and silver nitrite using an
60 elemental analyzer. ²

61 (ii) The denitrifier method uses bacterial strains with lacking nitrous oxide reductase activity to
62 stop the denitrification of nitrate and nitrite at N₂O, which is purified and trapped prior to IRMS
63 analysis. ³

64 (iii) The cadmium azide method uses a cadmium sponge to reduce nitrate to nitrite in a first
65 step and to further reduce nitrite to nitrous oxide prior to IRMS analysis. ⁴

66 (iv) Another method describes the measurement of ¹⁵N abundances of aqueous nitrate and
67 nitrite by on-line reduction to NO with vanadium or titanium chloride and subsequent
68 measurement with a membrane-inlet quadrupole MS (SPINS/MIMS) ⁵, based on a continuous-
69 flow mass spectrometry method developed in 1999. ⁶ This method has been improved over the
70 years ^{7,8} and the latest iteration uses an IRMS system instead of a quadrupole MS to measure
71 isotopic ratios directly. ^{9,10} Samples with a nitrogen concentration of 35 μmol L⁻¹ N for nitrate
72 can be measured and δ¹⁵N values from standards are reported with an accuracy of less than 0.9
73 ‰.

74 (v) Wassenaar, Altabet et al. developed a method based on the reduction to N₂O by reduction
75 with Ti(III) with subsequent cryogenic purification and detection by IRMS ¹¹ or without
76 purification by laser spectroscopy. ¹² The method provides the simultaneous measurement of
77 δ¹⁵N and δ¹⁸O by IRMS and δ¹⁷O values by laser spectroscopy.

78 (vi) Recently, Hilkert et al. showed that stable isotope ratio analysis (SIA) of nitrate is possible
79 using ESI Orbitrap. Nitrogen (δ¹⁵N_{AIR}), oxygen δ¹⁸O_{VSMOW}, and δ¹⁷O_{VSMOW} isotope ratios can
80 be measured simultaneously with a long-term precision of ≤ 0.4 ‰ for reference material and
81 purified nitrate samples. ¹³

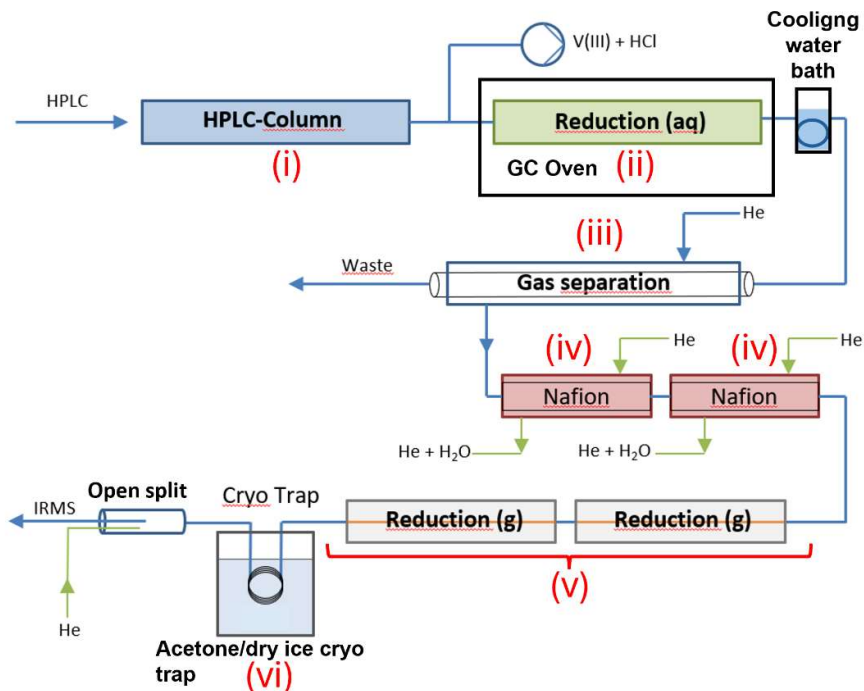
82 In order to develop an LC-IRMS method for the measurement of nitrogen isotope ratios from
83 organic compounds, one problem that had to be solved first was whether nitrogen species
84 formed during oxidation of organic compounds with peroxydisulfate that can be converted into
85 a measurable gas form such as N_2O , NO or N_2 .^{14,15} Our subsequent objective was therefore to
86 develop a method for measurement of nitrogen isotope signatures of nitrate through an online
87 conversion into gaseous nitrogen oxide species (N_xO_y) and subsequent reduction to elemental
88 nitrogen, while maintaining the capability for low-volume injections of samples. Furthermore,
89 the goal was to achieve a chromatographic separation of nitrate from the injection peak and
90 potentially nitrite. Here, we present the initial findings of standard sample measurements
91 conducted with the modified interface and discuss the method's limitations and possible options
92 for further improvement and future applications. Additionally, we had the opportunity to test
93 our system with samples from an enrichment experiment conducted in a small sandy river.

94 **2 Materials and Methods**

95 **2.1 Instrumental setup**

96 The instrument that we used in our initial proof-of-principle study was a modified commercially
97 available LC IsoLink™ interface (Thermo Fisher Scientific Inc., Bremen, Germany) (see
98 Figure 1). In a preliminary step (i), nitrate was chromatographically separated from the injection
99 peak and potential matrix interferences on a porous graphitic carbon (PGC)-HPLC column. In
100 a second step, nitrate was reduced by a $V(III)Cl_3$ solution to N_xO_y with nitric oxide (NO) being
101 the main product formed. Nitrogen oxides were separated from the eluent by membrane
102 pervaporation (iii). After Nafion™ drying (iv), N_xO_y and NO were reduced to N_2 gas by a
103 copper-filled ceramic reduction tube in a furnace (v).^{16,17} Furthermore, oxygen was scavenged
104 during this step, which enhances the precision and longevity of the filament in the IRMS ion
105 source. Following reduction to N_2 , carbon dioxide was removed by a cryo trap with a slurry of
106 acetone / dry ice (vi) before the N_2 entered the IRMS via an open split.

107

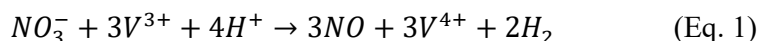


108

109 **Figure 1** Instrumental setup of the modified LC-IRMS for the determination of $\delta^{15}\text{N}$ isotope
 110 values of nitrate and nitrite. (i) Chromatographic separation of nitrate by ion chromatography,
 111 (ii) reduction to N_xO_y , (iii) gas separation unit, (iv) gas drying by two nafion dryer units, (v)
 112 reduction reactor, (vi) acetone/dry ice cryo trap to trap CO_2 . The nitrogen gas was introduced via
 113 an open split into the IRMS.

114 2.1 Chemicals and solutions

115 Vanadium(III)-chloride (97%, Merck, Darmstadt, Germany) was used to prepare solutions of
 116 0.015 M V(III)Cl_3 in 0.3 M HCl (36.5 % – 38%, Alfa Aesar, Kandel, Germany). In order to
 117 preserve the HPLC pumps, which were constructed from stainless steel and were susceptible to
 118 high chloride concentrations, we did not utilize excessive amounts of reducing agents. Heated
 119 hydrochloric acid is highly corrosive and can irreparably damage the stainless-steel reactor in
 120 the LC-IRMS interface, therefore a deactivated silica capillary was used (see below). The
 121 reduction of nitrate to nitric oxide with vanadium(III)-chloride follows the chemical reaction ⁵:



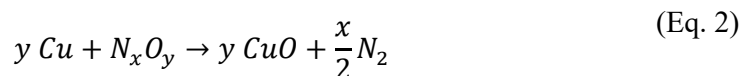
122 The reduction of nitrate to nitrogen oxide requires the presence of three parts of vanadium(III)
123 for every one part of nitrate. Therefore, a solution of 0.015 M VCl_3 is capable of reducing 0.005
124 M NO_3^- , which corresponds to a sample concentration of $140 \text{ mg L}^{-1} \text{NO}_3^-$. This concentration
125 can be injected into the system and completely reduced if we consider that the mobile phase
126 and reducing agents are mixed in a 1:1 ratio before they enter the reduction oven. The reduction
127 of nitrate with vanadium(III) requires strongly acidic conditions at or below $\text{pH } 1^{18}$, which was
128 provided by the 0.3 M HCl solution in which the vanadium(III)-chloride was solved. For
129 determination of conversion rates and selection of the acid see Supporting Information S 1 &
130 2. The solution was prepared with degassed Milli-Q water to avoid oxidation with dissolved
131 oxygen and stored in a refrigerator for up to one week. The eluent was prepared by diluting
132 sulfuric acid (95-97%, Merck, Darmstadt, Germany) to a concentration of 0.005 M H_2SO_4 or
133 to a concentration required for the experiment.

134 All solutions were subjected to further purification under vacuum by a membrane pump
135 (Vacuubrand GmbH & Co., Wertheim, Germany) and in an ultrasonic bath (Sonorex RK 100
136 Bandelin Electronic, Berlin, Germany) for a minimum of 15 minutes. They were continuously
137 flushed with a small flow of helium (5.0) (Air Liquide, Oberhausen, Germany) throughout their
138 use. The isotopic reference materials USGS 32, 34, and 35 (IVA Analysentechnik GmbH &
139 Co. KG, Meerbusch, Germany) and nitrate in-house standards KNO_3 and NaNO_3 (>99%,
140 Merck, Darmstadt, Germany) were measured on an Isoprime100 Elemental Analyzer
141 (Elementar Analysensysteme GmbH, Langenselbold, Germany) for referencing purposes. The
142 standard solutions typically contained $50 \text{ mg L}^{-1} \text{N-NO}_3^-$ (nitrate-N). One standard dilution
143 series was prepared with concentrations of 10, 25, 50, 75, and $100 \text{ mg L}^{-1} \text{N-NO}_3^-$ to assess the
144 concentration dependence of the system. For the determination of standard bulk isotope
145 signatures of the by EA-IRMS see Supporting Information 3.

146 **2.2 Experimental setup**

147 A scheme of the modified system is depicted in Figure 1. The modified system based on the
148 commercially available LC-Isolink interface (Thermo Fisher Scientific, Bremen, Germany)
149 coupled to a DELTA V Advantage IRMS (Thermo Fisher Scientific, Bremen, Germany) for
150 continuous flow applications. Eluents and reducing agents were pumped with two separate
151 HPLC pumps (LPG-3400 SD and HPG-3200 SD, Thermo Fisher Scientific, Bremen,
152 Germany). The flow rates for the eluent and reducing agents were both set to 200 $\mu\text{L min}^{-1}$.
153 Nitrate injections were performed by an HTC PAL autosampler (CTC Analytics AG, Zwingen,
154 Switzerland) with different sizes of PEEK sample loops (5, 10, and 20 μL). The separation of
155 nitrate from the injection peak and other potential matrix effects was achieved with a
156 HypercarbTM PGC column (2.1 x 100 mm, 3 μm , Thermo Fisher Scientific GmbH, Bremen,
157 Germany) and an eluent of 0.005 M H_2SO_4 . Furthermore, the column temperature was elevated
158 to 80°C and maintained by an HT-HPLC 200 column oven (Scientific Instruments
159 Manufacturer GmbH, Oberhausen, Germany) in order to enhance control over retention times
160 and peak shape. The reducing agent was introduced to the eluent via a corrosion free, low dead
161 volume mixing chamber integrated into the commercial LC-Isolink interface and pumped into
162 a heated deactivated fused silica capillary (i.d. 0.32 mm; length 8 m, BGB Analytik, Bökten,
163 Switzerland) for reduction. The dimensions of the fused silica capillary result in a reactor
164 volume of approximately 0.64 mL and a residence time of the analytes that is longer than 1.5
165 minutes, with a combined flow rate of 0.4 mL min^{-1} . Heating was facilitated by a small selfmade
166 temperature-controlled GC oven, which was controlled by an Eurotherm 2216e microprocessor
167 (Schneider Electric Systems, Limburg, Germany) (see Supporting Information 2 and Figure
168 2B). The mobile phase was cooled after reduction by immersing the capillary (20 cm length,
169 0.32 i.d.) BGBAnalytik, Bökten, Switzerland) in a water bath at RT (23°C) before entering the
170 gas separation unit of the Isolink LC-IRMS interface. A small inline filter made of 4.9 mm
171 diameter, 10 μm pore size, PEEKTM encased (IVA Analysentechnik & GmbH, Meerbusch,
172 Germany) was installed before the gas separation unit to shield the three membranes from

173 potential non-soluble particles. The analytes were extracted and transported by a helium stream
174 (Helium 5.0, Air Liquide, Oberhausen, Germany) of approximately 1–2 mL min⁻¹ through the
175 two Nafion™ membranes of the interface and into two subsequent heated copper reactors. Each
176 reactor consisted of four individual copper wires (length 28 cm; o.d. 0.125 mm) twisted and
177 inserted into a heated ceramic tube (length 320 mm; i.d. 0.5 mm) (both IVA Analytik,
178 Meerbusch, Germany). This tube was inserted into a custom-made GC oven, which was
179 controlled by two Jumo Itron16 (JUMO GmbH & Co. KG, Fulda, Germany) microprocessors
180 and held at 650°C. The copper reactor and subsequent CO₂ trap, a slurry of acetone / dry ice (-
181 78°C) for the LC-IRMS system, had been previously described in the literature ¹⁹ and served
182 several purposes. The copper reactor acted as an oxygen scrubber, that increased the lifetime
183 and precision of the filament. But it is of even greater significance in this context to note the
184 ability of heated copper to reduce gaseous nitrogen oxide species to elemental nitrogen in
185 accordance with the following equation:



186 The regeneration of the copper reactors was achieved by a stream of 3 % H₂ in He (Crystal
187 Mixture, Air Liquide Düsseldorf, Germany) at 3 – 4 mL min⁻¹.

188 **2.3 Test of reference gas stability**

189 The intensity of the reference gas peaks was controlled by adjusting the gas pressure of the
190 reference gas within the system using the pressure regulator of the interface. At the same time,
191 the sample inlet split on the LC-Isolink interface was opened while a 0.05 M H₂SO₄ eluent and
192 0.015 M VCl₃ in 0.3 M HCl reducing agent were pumped at a rate of 200 mL min⁻¹ each.

193 **2.4 Enrichment experiment**

194 The Rotbach River is a minor tributary of the Rhine in western Germany (51.5724°N 6.6871°E).
195 The enrichment with heavy nitrogen (¹⁵N) was carried out by using isotopically enriched

196 $^{15}\text{NH}_4\text{Cl}$ (Silantes, minimum 99 atom. % ^{15}N purity). It was diluted in 40 L distilled water for
197 each enrichment experiment. This tracer solution was released via a Duran glass Mariotte's
198 bottle (Schott, Mainz, Germany) which assured a consistent release of the solution independent
199 of the hydrostatic pressure within the bottle. In May and June 2021, a bottle of the labeled
200 material was exposed to the river in order to allow a constant portion to leach into the stream
201 over the course of six weeks. Water samples were collected at designated locations on a weekly
202 basis at distances of 50, 100, 200, 300, 500, 750, 1000, 1500, and 2000 meters downstream
203 from the administration point. Additionally, one sample was collected 50 meters upstream as a
204 reference. The samples were subsequently frozen and stored until further analysis. Given that
205 the modified LC-IsolinkTM interface was not suitable for direct injection and measurement of
206 nitrate from water samples, we proceeded to pre-concentrate the water samples after thawing
207 in a vacuum evaporator. This involved evaporating 50 mL of each water sample at 60°C and
208 under 50 mbar to approximately 1 mL, thereby enriching the samples by a factor of 50. Separate
209 spectroscopic measurements of ammonium, nitrite, and nitrate (Tabel S6) demonstrated that the
210 nitrate concentration in the river was approximately 7 mg L⁻¹, which corresponds to 1.58 mg L⁻¹
211 ¹⁵N. Enriching the nitrate concentration by vacuum evaporation 50-fold would result in a
212 concentration of ~80 mg L⁻¹ ¹⁵N, which should fall within the previously determined
213 measurement range of the modified interface. Although the system still exhibits a non-linear
214 shift in $\delta^{15}\text{N}$ values and peak areas, this shift should not impede the ability to detect enriched
215 nitrogen isotope signatures. We proceeded to evaporate and measure a 1:50 diluted sample of
216 the in-house standard at an initial concentration of 50 mg L⁻¹ ¹⁵N. This was done to ascertain the
217 impact of isotope fractionation effects during evaporation. Following evaporation, all samples
218 were filtered through 0.2 μm PTFE filters (FisherScientific, Schwerte, Germany), and 10 μL of
219 the resulting sample volume was directly injected into the system.

220 **3 Results and Discussion**

221 3.1 Stability and linearity of IRMS under measurement conditions

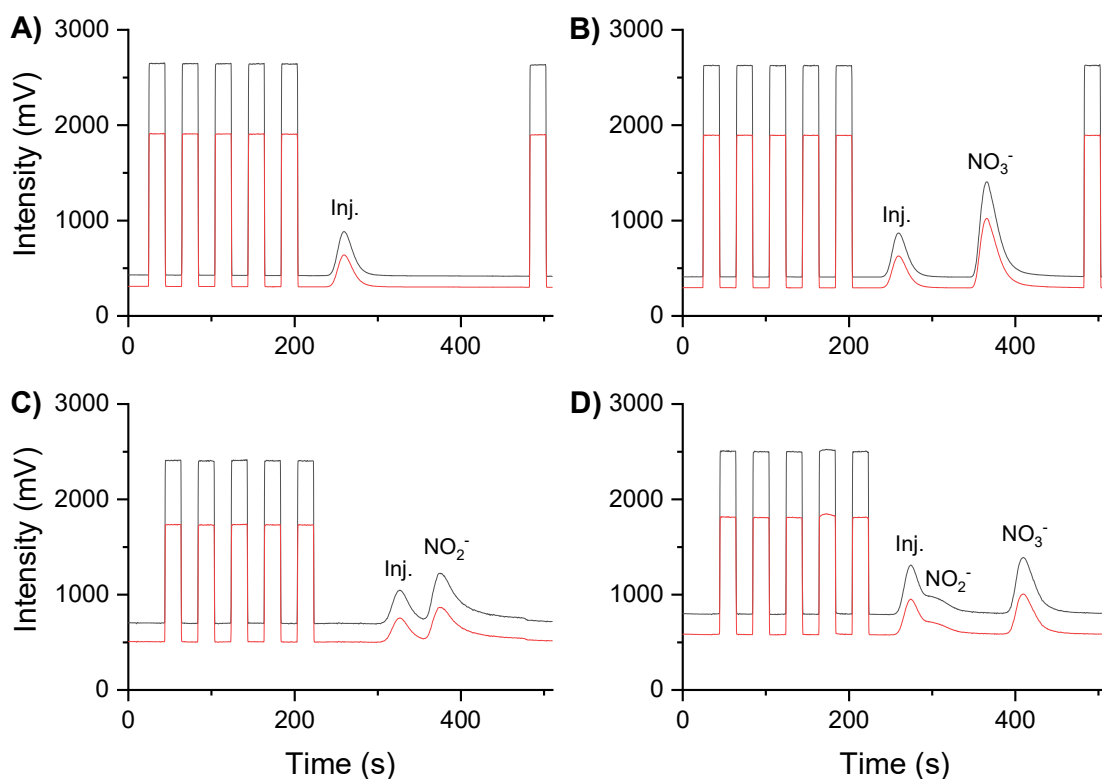
222 In order to assess the precision of the IRMS system for nitrogen isotope signatures under
223 measurement conditions, ten consecutive reference gas peaks were injected with constant
224 (stability) and increasing (linearity) signal intensities. Table S2 presents the average (Avg) and
225 standard deviation (SD) of $\delta^{15}\text{N}$ values from ten reference gas peaks (denoted by w). These
226 values were compared to linearity measurements without background signals, whereby the
227 sample open split was turned off (denoted by $w\phi$). The SD of linearity measurements of nitrogen
228 isotope signatures without any background signals under ideal IRMS conditions was 0.06 ‰
229 and increased to 0.41 ‰ conducting the same measurements with an active sample open split.
230 The SD of stability measurements with an active sample open split (w) was 0.37 ‰. The main
231 cause for the increasing SD of measurements with an active open split were outliers (peak no.
232 6 for linearity and peak no. 4 for stability measurements, marked with * in Table S2) throughout
233 the complete series of ten reference gas injections. The cause for these outliers were small shifts
234 in the m/z 29/28 ratios (see Supporting Information Figure S4) occasionally appearing
235 throughout chromatograms. The shifts tend to be one-minute-long and, due to the nature of the
236 interface to produce wide peaks, they might originate from the liquid phase of the system,
237 possibly due to piston movement of the HPLC pumps. We took great care to manually check
238 and avoid measurements where one of these shifts occurred under peaks of interest. Despite
239 these interferences, the system performs sufficiently robust and is able to measure nitrogen
240 isotope signatures of elemental nitrogen with a precision better than 0.5 ‰ over a peak area
241 range of 4.6 to 21.3 Vs and possibly more precise if background shifts are avoided.

242 3.2 Separation of nitrate and nitrite from injection peak

243 Blank injections into the modified interface produced significant nitrogen peaks (Figure 2A),
244 which also occurred with no reducing agents in the mobile phase and when the reactors were at
245 room temperature. The measured $\delta^{15}\text{N}$ signatures of these peaks were between +2 and +8‰

246 against the nitrogen reference gas, which was set to zero. We therefore assumed that these blank
247 peaks were either produced by dissolved elemental nitrogen in the sample or by switching the
248 valve position of the 6-port valve from the autosampler. Switching the valves might have
249 introduced small amounts of elemental nitrogen from the surrounding air into the eluent flow
250 of the system. Separation of nitrate from the injection peak and nitrite was therefore crucial to
251 avoid interferences and was achieved by a porous graphitic carbon (PGC) HPLC column
252 (Hypercarb 100 x 2.1 mm, 5 μm , ThermoScientific). We used an elevated column temperatures
253 at around 80°C and diluted sulfuric acid as anionic competitor to elute nitrate from the column.
254 Without an anionic competitor, nitrate would be totally retained on the column. Sodium sulfate
255 was used by Takeuchi et al. to separate inorganic anions including nitrate and nitrite on a PGC
256 column²⁰, but we decided to use diluted sulfuric acid (0.005 M H_2SO_4) instead to keep the pH
257 as low as possible for subsequent reduction (pH \sim 1). However, due to the broad peak widths
258 produced in our modified interface and the LC-IRMS interface in general, efficient separation
259 of nitrite and nitrate from the injection peak was not possible simultaneously (Figure 2B). Here,
260 the HPLC flow was set to 200 μLmin^{-1} for both the eluent and reducing agent (0.03 M VCl_3 in
261 0.3 M HCl) and reactor column temperature was held at 55°C. Since the focus of this work was
262 the measurement of nitrogen isotope signatures from nitrate, separation of nitrate from both
263 blank and nitrite peaks was considered sufficient. Injecting a mixture of nitrate and nitrite (50
264 mgL^{-1} N each, 5 μL injection volume) under these flow conditions (Figure 2D) showed that
265 nitrite was not fully separated from the injection peak. Reducing the eluent flow from 200 to
266 150 μLmin^{-1} and increasing the column temperature to 80°C (Figure 2C) almost separated
267 nitrite (100 mg L^{-1} N, 5 μL injection volume) from the injection peak. Note that the injection
268 volume was reduced from initially 10 μL (A and B) to 5 μL (Figure 2C and D) to reduce the
269 load of nitrogen oxides on the copper reactor. The concentration of sulfate in the eluent, flow
270 rates and column temperatures can be used to influence the retention time of nitrate, which is
271 not only useful to control the to avoid possible matrix interferences or baseline fluctuations in

272 real samples. Testing different column parameters and materials might result in an improved
273 performance of the system to separate both nitrate and nitrite from the injection peak.



274

275 **Figure 2** Chromatograms of blank (A), nitrate (B), nitrite (C) and a mix of both nitrate/nitrite (D)
276 injections into the modified LC-IRMS interface for the measurement of nitrogen isotope signatures.
277 Blank injections produce a measurable nitrogen peak (A).

278 3.3 Repeated nitrate measurements and reactor performance

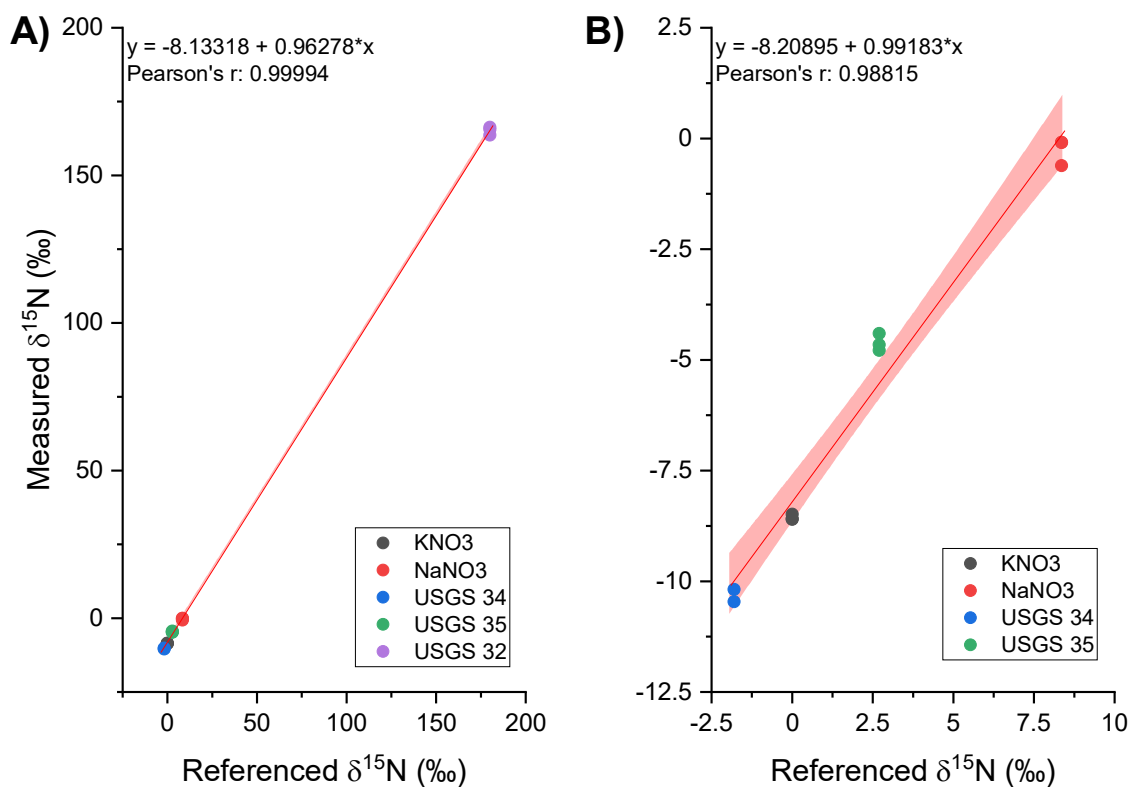
279 To evaluate the ability of the copper reactor to reduce the high loads of nitrogen oxides coming
280 from the modified LC-IRMS interface in addition to the oxygen loads coming from the eluent,
281 we consecutively injected 5 μL of a 50 mgL^{-1} N solution of the USGS 34 international reference
282 material on three following days. The copper reactor was reduced overnight in between
283 measurement days with a 2 mL min^{-1} flow of 3 vol-% H_2 in He gas. The measured $\delta^{15}\text{N}$ values
284 were constant for four to six injections, after which they started to decrease until the 20th to 25th
285 injection (see Figure S5). This indicated that the reactor performance is stable for the first few
286 injections, but quickly declines afterwards. Overnight regeneration of the reactor increased the
287 measured $\delta^{15}\text{N}$ values on the next day, but not to the same values previously observed. This

288 showed that while regenerating the reactor is feasible, there might still be daily differences in
289 reactor or system performance. Thus, frequent referencing through international or in-house
290 standards, as typically required and practiced in CSIA, minimized the daily influence on the
291 performance. Measuring nitrogen isotope ratios from nitrate with high precision throughout a
292 day or for prolonged sample runs might therefore require a combination of two copper reactors
293 in parallel, where one reactor is used for one or several injections of nitrate containing samples
294 while the other is regenerated with a separate line of hydrogen gas.

295 **3.4 Measuring different nitrogen reference materials with a wide range of isotopic signatures**

296 Two international nitrate reference materials with certified nitrogen isotope signatures on
297 natural abundance levels (USGS 34 and USGS 35) and one material enriched in its nitrogen
298 isotope ratio (USGS 32) were utilized in this study. Additionally, two in-house nitrate standards
299 (KNO_3 and NaNO_3) were calibrated on an EA-IRMS system with the three USGS reference
300 materials. The referenced values of all five standard and reference materials are summarized in
301 Table S1. We injected 10 μL of a nitrate solution containing 50 mg L^{-1} N-NO_3^- of each material
302 in triplicate and plotted the measured $\delta^{15}\text{N}$ values with all standard and reference materials
303 (Figure 3A) and with materials on natural abundance levels (Figure 3B). The y-intercept of a
304 linear regression curve between referenced and measured $\delta^{15}\text{N}$ values shows that measured $\delta^{15}\text{N}$
305 values are -8.1 and -8.2 ‰ lower than the referenced values, but a slope of 0.96 and 0.99
306 indicates that the differences between measured values of different materials are in good
307 agreement to the differences of referenced values. As mentioned earlier, we occasionally
308 observed small shifts in the m/z 29/28 ratio during measurements, which resulted in higher
309 measured $\delta^{15}\text{N}$ values if the shifts overlapped with either a reference gas peak or a
310 chromatographic peak and caused the observed difference. The reported values were produced
311 throughout continuous measurements on two individual days and the copper reactors were
312 regenerated overnight. The results are therefore also subject to isotope shifts over extended

313 measurement periods and to different copper reactor performance on individual sampling days.
314 Addressing these issues might therefore further improve the precision and linearity of the
315 regression. However, the reported values already show that the measurement of nitrogen isotope
316 signatures from nitrate with the current setup was feasible on both natural and enriched
317 abundance levels.



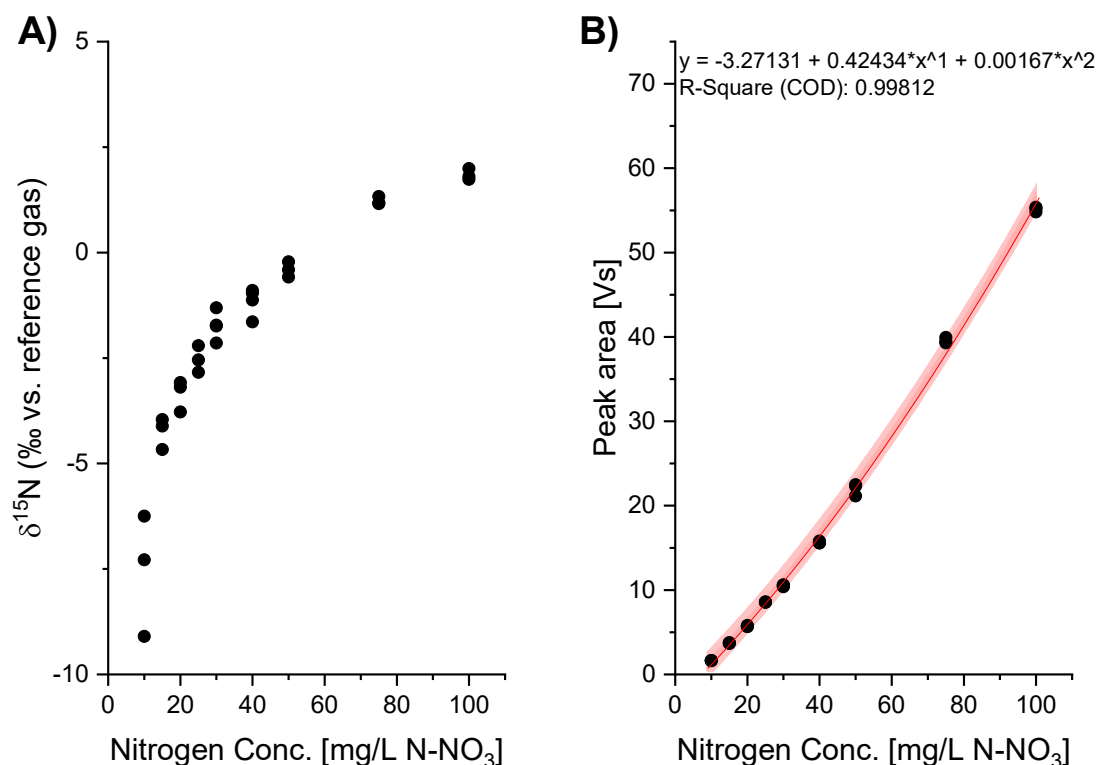
318

319 **Figure 3** Differences between measured and referenced $\delta^{15}\text{N}$ values of reference materials and in-house
320 standards were in good agreement. Since USGS 32 is an enriched reference material (A), it was removed
321 for the linear regression (B) to decrease the range of $\delta^{15}\text{N}$ values to more natural abundance levels. Red
322 line indicates linear regression curve and red area gives the 95% confidence interval. Samples were
323 injected in triplicates.

324 3.5 Measuring different nitrate concentrations

325 To test the influence of nitrate concentration on nitrogen isotope signatures of nitrate, we
326 prepared and measured a dilution series of NaNO₃ in-house standards. 10 μL injections of
327 different N-NaNO₃ solution concentrations were done in triplicate and the measured $\delta^{15}\text{N}$
328 values and peak areas were plotted against the nitrogen concentration (Figure 4A & B). $\delta^{15}\text{N}$
329 values increase non-linear from -7.5 ± 1.4 ‰ to $+1.8 \pm 0.1$ ‰ over a range of 10 to 100 mgL^{-1}
330 N-NaNO₃ while peak areas simultaneously increase non-linear from 1.6 ± 0.0 Vs to 55.1 ± 0.3

331 Vs and are best described by a second order polynomial equation with a Pearson coeff. r of
332 0.998. The measured $\delta^{15}\text{N}$ values of $50\text{ mg L}^{-1}\text{ N-NaNO}_3$ was $-0.4 \pm 0.2\text{ ‰}$. The lowest injected
333 nitrate concentration of $10\text{ mg L}^{-1}\text{ N}$ shows a noticeable increase in measurement uncertainty
334 and the largest shift of $\delta^{15}\text{N}$ values. However, $\delta^{15}\text{N}$ values were stable once a concentration of
335 $100\text{ mg L}^{-1}\text{ N-NaNO}_3$ was reached and peak areas showed a linear increase from 50 mg L^{-1}
336 onwards. These concentrations are about 10 to 50 times higher than what is usually observed in
337 water samples from areas affected by substantial agricultural activities, which results in nitrate
338 concentrations between 10 and $50\text{ mg/L}^{-1}\text{ N-NO}_3^-$.²¹ Especially, nitrate concentration in
339 groundwaters or areas with limited agricultural activities were below the currently expected
340 detection limits of the modified interface. As mentioned earlier, increasing the injection volume
341 is a potential way of achieving the necessary analyte amount on the column if chromatographic
342 separation is assured and the column is not overloaded. However, in our current set-up, sample
343 enrichment prior to injection was necessary. Such an enrichment could be achieved by
344 evaporation under vacuum (see next section) or by the use of anion exchange columns to
345 preconcentrate nitrate, as described by the ion-exchange method.²



346

347 **Figure 4** Injection of nitrate in different concentrations leads to a shift of measured $\delta^{15}\text{N}$ values (A) and
348 a non-linear increase in peak areas (B). $10\text{ }\mu\text{L}$ NaNO_3 solutions from 10 to $100\text{ mg/L}^{-1}\text{ N-NO}_3$ were
349 injected in triplicate and the $\delta^{15}\text{N}$ values (‰) and peak area (Vs) measured. Peak integration was done
350 by ISODAT software with the default settings of 0.2 and 0.4 mV s^{-1} start and end slope detection and

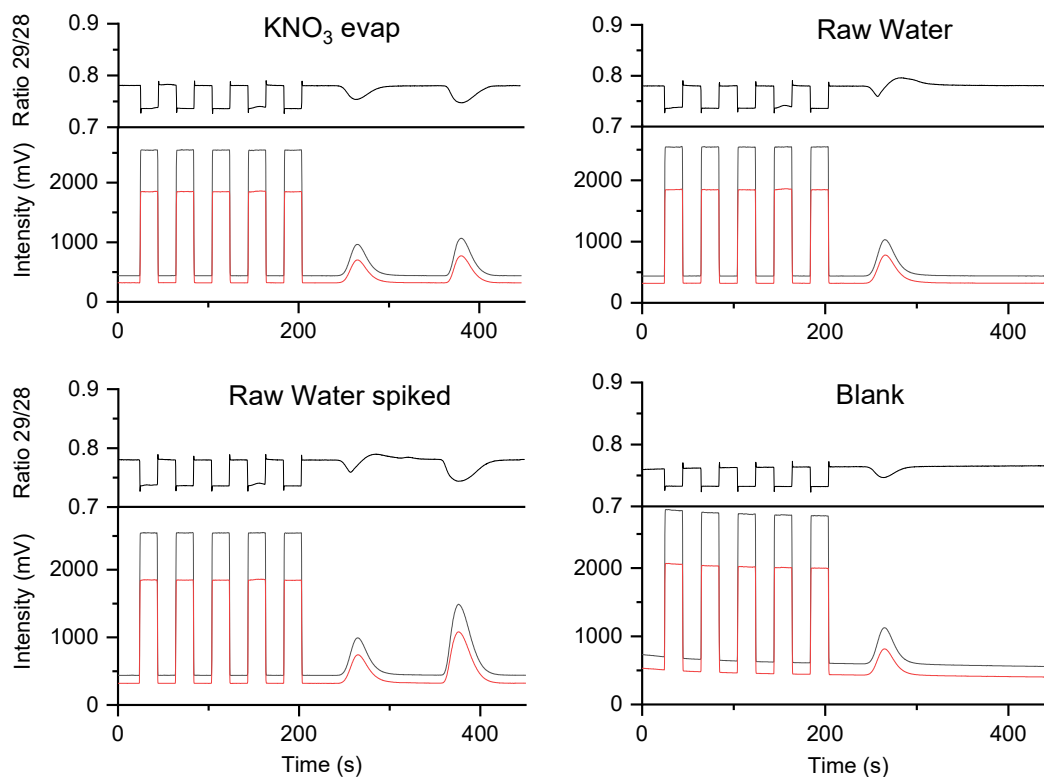
351 an individual background detection algorithm with a 5 second history. The increase in peak area over
352 the concentration range is best described by a second polynomial equation with R-Square of 0.998.

353 **3.6 Sample evaporation, blank samples and raw river water**

354 In our study, we decided to test and employ sample evaporation to increase the nitrate
355 concentration in real water samples. Injections of 10 μL MilliQ water (blank) into the system
356 show blank peaks of dissolved nitrogen gas in the IRMS system after 260 s under the employed
357 conditions, which had $\delta^{15}\text{N}$ values between +4 ‰ and +10 ‰ measured against the reference
358 gas. No nitrate peak was visible in blank samples (Figure 5 bottom right). To test if evaporation
359 of a nitrate solution leads to isotope fractionation, we diluted (1:50) standard solutions of 50
360 mg L^{-1} KNO_3 and 25 mg L^{-1} NaNO_3 and evaporated 50 mL down to 1 mL sample volume.
361 Injecting 10 μL of the evaporated standard solutions and measuring the nitrogen isotope
362 signature showed no significant difference in $\delta^{15}\text{N}$ values compared to non-evaporated standard
363 samples (Welch's t-tests, $t_2 = -2.488$, $p = 0.124$ for NaNO_3 and $t_2 = 0.257$, $p = 0.821$ for KNO_3).
364 The reported standard deviations for evaporated standard solutions were noticeable higher (1.7
365 ‰ for KNO_3 and 1.2 ‰ for NaNO_3) compared to normal standard solutions (0.2 ‰ for both
366 KNO_3 and NaNO_3). Injecting raw river water from an isotopic enrichment experiment with
367 $^{15}\text{NH}_4\text{Cl}$, which was not evaporated to pre-concentrate nitrate, also showed an injection peak
368 after 265 s and no measurable nitrate peak (Figure 5 top right). The injection peak from ^{15}N -
369 enriched raw water samples, however, exhibited a visible positive shift in m/z 29/28 ratios
370 leading to an increased $\delta^{15}\text{N}$ value of $+91.0 \pm 2.5$ ‰. The observed positive shift appeared not
371 immediately with the beginning of the peak, where signal intensities start to rise, but shortly
372 afterwards before the peak intensity reached its maximum. Spiking a raw water sample with
373 nitrate in-house standards resulted in a nitrate peak after 376.2 s, while the positive isotope shift
374 during the injection peak remained. The injection peaks of evaporated standard solutions further
375 did not exhibit the unusual positive shift of the m/z 29/28 ratio observed in ^{15}N -enriched raw

376 water samples and the $\delta^{15}\text{N}$ values of the injection peaks remained under 10 ‰ and comparable
377 to blank or regular standard solutions.

378



379

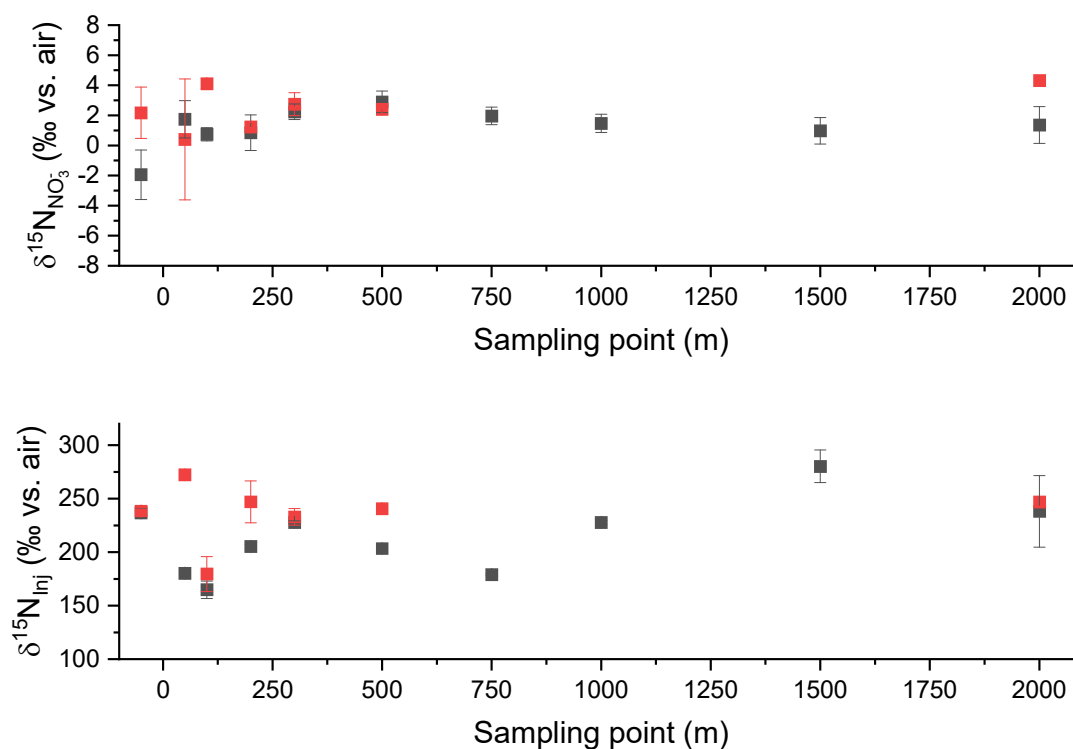
380 **Figure 5:** Chromatograms show measurements of evaporated KNO₃ standard solutions (top left), river
381 water (top right), river water spiked with a nitrate standard (bottom left) and a blank sample of
382 evaporated MilliQ water (bottom right). Evaporation overnight in a vacuum evaporator does not
383 influence the m/z 29/28 ratio of either the nitrate peak (around 380 s) or injection peaks.

384

385 3.7 River samples from an enriched ammonium chloride administration experiment

386 The measured nitrate concentrations in the river Rotbach were between 6 to 8 mg L⁻¹ (see Table
387 S6) and the resulting nitrogen concentrations were around 1.2 mg L⁻¹ N-NO₃⁻, which could not
388 be measured directly due to low sensitivity. Thus, we measured the nitrogen isotope signature
389 of N-NO₃⁻ from concentrated river water one and two weeks after administration of isotopically
390 enriched ammonium chloride. In contrast to expectations, $\delta^{15}\text{N}$ values of river nitrate stayed
391 between $+0.4 \pm 0.4$ ‰ and $+4.1 \pm 0.3$ ‰ in those two weeks, varying over a small range of 3.7

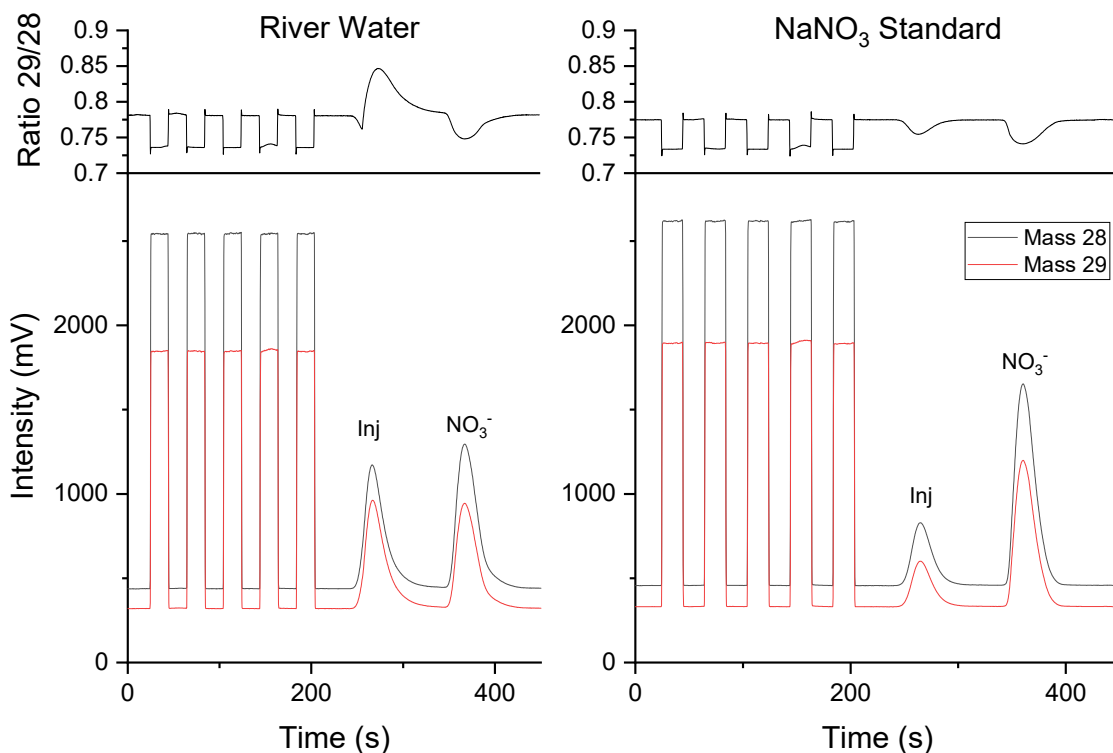
392 ‰ (Table S5). No trends in $\delta^{15}\text{N}$ values were observed between sampling points or between
393 sampling weeks (see Figure 6). After the second week, the reference point had a $\delta^{15}\text{N}$ value of
394 $+2.2 \pm 1.7$ ‰, which was well within the observed range of $\delta^{15}\text{N}$ values of nitrate downstream
395 the administration point.



396 **Figure 6:** Nitrogen isotope signatures (‰ vs Air) of nitrate (NO_3^- , top) and the injection peak (Inj.,
397 bottom) from evaporated water samples of the river Rotbach after one week (grey boxed) and two weeks
398 (red boxes) of introducing isotopically enriched ammonium chloride. Samples were taken up to 2000 m
399 downstream of the administration point and one sample 50 m upstream as a reference.
400

401

402 The $\delta^{15}\text{N}$ values of the injection peaks for all samples during that time were much higher and
403 ranged between $+164.8 \pm 8.1$ ‰ and $+272.4 \pm 1.2$ ‰, but also with no observable trend either
404 between sampling points or weeks. The chromatograms of evaporated river water showed
405 highly enriched compound eluting from the column right after the start of the injection peak
406 (see Figure 7), as the m/z 29/28 ratio showed a strong positive shift shortly after the beginning
407 of the chromatographic peak, which was comparable to what we also observed in non-
408 evaporated water samples.



409

410 **Figure 7** Chromatogram of evaporated river water (left) and NaNO₃ standard solution at 50
 411 mgL⁻¹ N-NO₃⁻ (right) showing separation of nitrate from the injection peak. Lines in the bottom
 412 section represent signal intensities (mV) of m/z 28 (black) and 29 (red) for the determination
 413 of $\delta^{15}\text{N}$ values by the IRMS. The upper sections show the ratio of m/z 29/28 intensities and
 414 reveal an unusual swing in the injection peak for the river water sample, which is typically not
 415 observed.

416

417 The isotope swing observed in raw water samples during the injection peak represents an
 418 interesting result, leading to highly increased $\delta^{15}\text{N}$ values of the injection peak around ~90 ‰.
 419 This indicates that either the atmospheric nitrogen in the river water is highly enriched in ¹⁵N
 420 or some enriched nitrogen oxide species are present in the sample, which are subsequently
 421 reduced and measured as elemental nitrogen in the IRMS. The first possibility might be
 422 unlikely, since the isotope swing does not completely overlap with the nitrogen injection peak
 423 and has a small offset before the positive shift in m/z 29/28 ratio occurs. This would indicate
 424 that the observed isotope swing during the injection peak of raw river water is caused by partial
 425 coelution of isotopically enriched nitrite. The abundance of nitrite in river water is two orders

426 of magnitude lower compared to nitrate, which means that the isotope composition of nitrite in
427 the water sample would be much higher than the measured $\delta^{15}\text{N}$ value of $\sim 90\%$, since it
428 coelutes with the much more abundant nitrogen injection peak and typically has a $\delta^{15}\text{N}$ value
429 of $\sim 5\%$. This is supported by measurements of evaporated river water, where the $\delta^{15}\text{N}$ value
430 of the injection peak is even higher and reaches over $+200\%$, which would be a direct result
431 of concentration of nitrite alongside nitrate in the sample material. In case of the administration
432 study, our results suggest that concentration of nitrate in water samples via evaporation under
433 vacuum is feasible without isotope fractionation and the measured $\delta^{15}\text{N}$ values of evaporated
434 as well as non-evaporated nitrate standards are statistically not distinguishable.

435 **Conclusions**

436 In this study we presented a modified LC-IRMS interface for the measurement of nitrogen
437 isotope signatures of nitrate from aqueous solutions. Chromatographic separation of nitrate
438 from other nitrogen containing compounds and consecutive reduction to elemental nitrogen was
439 achieved and nitrogen isotope signatures were measured from injections from up to $20\ \mu\text{L}$
440 aqueous samples. We accomplished chromatographic separation of nitrate from blank peaks to
441 increase accuracy and decrease matrix interferences.

442 Under current conditions, measurements of in-house standards and reference materials showed
443 that the linearity of measured $\delta^{15}\text{N}$ values were in good agreement with both literature and
444 referenced $\delta^{15}\text{N}$ values from an EA-IRMS system. Because of the early state of the modified
445 system, this study can be interpreted as a proof of principle. Major challenges that should be
446 addressed in the future include (i) reducing the nitrogen background from the eluent, (ii)
447 modifying the copper reactors to operate in parallel to enable simultaneous regeneration of
448 oxidized copper wires and (iii) reducing peak broadening by testing different column materials
449 and optimizing flow conditions both in the liquid and gas phase. In addition, positioning of the
450 switching valve heads into a nitrogen free gas atmosphere could reduce the amount of air

451 entering the system. These modifications will likely address the observed issues of low
452 sensitivities as well as drifting isotope signatures over time. A separation and measurement of
453 both nitrite and nitrate with one measurement might be possible if separation with other HPLC
454 columns can be optimized.

455 **Acknowledgements**

456 This study was performed within the Collaborative Research Center (CRC) RESIST funded by
457 the Deutsche Forschungsgemeinschaft (DFG, German Research Foundation) – CRC 1439/1 –
458 project number: 426547801. Additionally, the research was funded by the German Research
459 Foundation (DFG) under the project grants 278676953 and 317438550.

460 **Declaration of competing interest**

461 The authors declare that they have no known competing financial interests or personal
462 relationships that could have appeared to influence the work reported in this paper.

463 **Authorship contribution statement**

464 **Tobias Hesse** Methodology, Sampling Formal analysis, Investigation, Visualization, Writing -
465 Original Draft. **Felix Niemann**: Sampling Formal analysis, Investigation, Review & Editing.
466 **Shaista Khaliq**: Sampling Formal analysis, Review & Editing. **Daniel Köster**:
467 Conceptualization, Methodology. **Julian Enss**: Sampling, Review & Editing. **Christian K.**
468 **Feld**: Sampling, Review & Editing. **Milen Nachev**: Sampling, Review & Editing. **Klaus**
469 **Kerpen**: Investigation. **Maik A. Jochmann**: Conceptualization, Methodology, Writing -
470 Review & Editing, Supervision. **Torsten C. Schmidt**: Conceptualization, Methodology,
471 Writing - Review & Editing Supervision.

472

473 **Literature**

474

- 475 1. Xia XH, Yang ZF, Huang GH, Zhang XQ, Yu H, Rong X. Nitrification in natural waters with
476 high suspended-solid content--a study for the Yellow River. *Chemosphere*. 2004;57(8):1017-
477 1029.DOI:10.1016/j.chemosphere.2004.08.027.
- 478 2. Silva SR, Kendall C, Wilkison DH, Ziegler AC, Chang CCY. A new method for collection of
479 nitrate from fresh water and the analysis of nitrogen and oxygen isotope ratios. *Journal of*
480 *Hydrology*. 2000;228:22-36.DOI:10.1016/S0022-1694(99)00205-X.
- 481 3. Sigman DM, Casciotti KL, Andreani M, Barford C, Galanter M, Böhlke JK. A Bacterial
482 Method for the Nitrogen Isotopic Analysis of Nitrate in Seawater and Freshwater. *Anal Chem*.
483 2001;73(4145-4153).DOI:10.1021/ac010088e.
- 484 4. McIlvin MR, Altabet MA. Chemical Conversion of Nitrate and Nitrite to Nitrous Oxide for
485 Nitrogen and Oxygen Isotopic Analysis in Freshwater and Seawater. *Anal Chem*.
486 2005;77:5589-5595.DOI:10.1021/ac050528s.
- 487 5. Stange CF, Spott O, Apelt B, Russow RW. Automated and rapid online determination of ¹⁵N
488 abundance and concentration of ammonium, nitrite, or nitrate in aqueous samples by the
489 SPINMAS technique. *Isotopes Environ Health Stud*. 2007;43(3):227-
490 236.DOI:10.1080/10256010701550658.
- 491 6. Russow R. Determination of ¹⁵N in ¹⁵N-Enriched Nitrite and Nitrate in Aqueous Samples by
492 Reaction Continuous-flow Quadrupole Mass Spectrometry. *Rapid Commun Mass Spectrom*.
493 1999;13:1334-1338.DOI:10.1002/(SICI)1097-0231(19990715)13:13<1334::AID-
494 RCM606>3.0.CO;2-C.
- 495 7. Eschenbach W, Lewicka-Szczebak D, Stange CF, Dyckmans J, Well R. Measuring (¹⁵N)
496 Abundance and Concentration of Aqueous Nitrate, Nitrite, and Ammonium by Membrane
497 Inlet Quadrupole Mass Spectrometry. *Anal Chem*. 2017;89(11):6076-
498 6081.DOI:10.1021/acs.analchem.7b00724.
- 499 8. Eschenbach W, Well R, Dyckmans J. NO Reduction to N₂O Improves Nitrate (¹⁵N)
500 Abundance Analysis by Membrane Inlet Quadrupole Mass Spectrometry. *Anal Chem*.
501 2018;90(19):11216-11218.DOI:10.1021/acs.analchem.8b02956.
- 502 9. Dyckmans J, Eschenbach W, Langel R, Szwec L, Well R. Nitrogen isotope analysis of
503 aqueous ammonium and nitrate by membrane inlet isotope ratio mass spectrometry (MIRMS)
504 at natural abundance levels. *Rapid Commun Mass Spectrom*.
505 2021;35(10):e9077.DOI:10.1002/rcm.9077.
- 506 10. Huang K, Eschenbach W, Wei J, et al. Simultaneous ¹⁵N Online Analysis in NH₄⁺, NO₂⁻,
507 NO₃⁻, and N₂O to Trace N₂O Production Pathways in Nitrogen-Polluted Aqueous
508 Environments. *ACS ES&T Water*. 2023;3(11):3485-3495.10.1021/acsestwater.3c00216.
- 509 11. Altabet MA, Wassenaar LI, Douence C, Roy R. A Ti(III) reduction method for one-step
510 conversion of seawater and freshwater nitrate into N₂O for stable isotopic analysis of
511 ¹⁵N/¹⁴N, ¹⁸O/¹⁶O and ¹⁷O/¹⁶O. *Rapid Communications in Mass Spectrometry*.
512 2019;33(15):1227-1239.DOI:10.1002/rcm.8454.
- 513 12. Wassenaar LI, Douence C, Fortson S, Baer DS. Automated rapid triple-isotope ($\delta^{15}\text{N}$, $\delta^{18}\text{O}$,
514 $\delta^{17}\text{O}$) analyses of nitrate by Ti(III) reduction and N₂O laser spectrometry. *Isotopes in*
515 *Environmental and Health Studies*. 2023;59(3):297-
516 308.DOI:10.1080/10256016.2023.2222222.
- 517 13. Hilker A, Böhlke JK, Mroczkowski SJ, et al. Exploring the Potential of Electrospray-Orbitrap
518 for Stable Isotope Analysis Using Nitrate as a Model. *Analytical Chemistry*.
519 2021;93(26):9139-9148.DOI:10.1021/acs.analchem.1c00944.
- 520 14. Köster D, Jochmann MA, Lutze HV, Schmidt TC. Monitoring of the total carbon and nitrogen
521 balance during the mineralization of nitrogen containing compounds by heat activated
522 persulfate. *Chemical Engineering Journal*. 2019;367:160-168.DOI:10.1016/j.cej.2019.02.115.
- 523 15. Köster D, Sanchez Villalobos IM, Jochmann MA, Brand WA, Schmidt TC. New Concepts for
524 the Determination of Oxidation Efficiencies in Liquid Chromatography-Isotope Ratio Mass
525 Spectrometry. *Anal Chem*. 2019;91(8):5067-5073.DOI:10.1021/acs.analchem.8b05315.
- 526 16. Brand WA. High precision isotope ratio monitoring techniques in mass spectrometry. *Journal*
527 *of Mass Spectrometry*. 1996;31(3):225-235.DOI:10.1002/(sici)1096-
528 9888(199603)31:3<225::aid-jms319>3.0.co;2-l.

- 529 17. Merritt SA, Hayes JM. Nitrogen Isotopic Analyses by Isotope-RatioMonitoring Gas
530 Chromatography/ Mass Spectrometry. *J Am Soc Mass Spectrom.* 1994;5:387-
531 397.DOI:10.1016/1044-0305(94)85054-2
- 532 18. Braman RS, Hendrix SA. Nanogram nitrite and nitrate determination in environmental and
533 biological materials by vanadium (III) reduction with chemiluminescence detection.
534 *Analytical chemistry.* 1989;61(24):2715-2718.DOI:10.1021/ac00199a007
- 535 19. Hettmann E, Brand WA, Gleixner G. Improved isotope ratio measurement performance in
536 liquid chromatography/isotope ratio mass spectrometry by removing excess oxygen. *Rapid*
537 *Commun Mass Spectrom.* 2007;21(24):4135-4141.DOI:10.1002/rcm.3304.
- 538 20. Takeuchi T, Kojima T, Miwa T. Ion chromatography of inorganic anions on graphitic carbon
539 as the stationary phase. *Journal of High Resolution Chromatography.* 2000;23(10):590-
540 594.DOI:10.1002/1521-4168(20001001)23:10<590::AID-JHRC590>3.0.CO;2-C.
- 541 21. He B, Kanae S, Oki T, Hirabayashi Y, Yamashiki Y, Takara K. Assessment of global nitrogen
542 pollution in rivers using an integrated biogeochemical modeling framework. *Water Res.*
543 2011;45(8):2573-2586.DOI:10.1016/j.watres.2011.02.011.
- 544